

## Cross section measurements of deuteron induced nuclear reactions on natural titanium up to 34 MeV

C. Duchemin, Arnaud Guertin, Ferid Haddad, Nathalie Michel, Vincent Métivier

### ► To cite this version:

C. Duchemin, Arnaud Guertin, Ferid Haddad, Nathalie Michel, Vincent Métivier. Cross section measurements of deuteron induced nuclear reactions on natural titanium up to 34 MeV. Applied Radiation and Isotopes, Elsevier, 2015, 103, pp.160-165. 10.1016/j.apradiso.2015.06.014. in2p3-01188673

**HAL Id: in2p3-01188673**

**<http://hal.in2p3.fr/in2p3-01188673>**

Submitted on 26 Jan 2021

**HAL** is a multi-disciplinary open access archive for the deposit and dissemination of scientific research documents, whether they are published or not. The documents may come from teaching and research institutions in France or abroad, or from public or private research centers.

L'archive ouverte pluridisciplinaire **HAL**, est destinée au dépôt et à la diffusion de documents scientifiques de niveau recherche, publiés ou non, émanant des établissements d'enseignement et de recherche français ou étrangers, des laboratoires publics ou privés.

# Cross Section Measurements of Deuteron Induced Nuclear Reactions on Natural Titanium up to 34 MeV

C. Duchemin<sup>a</sup>, A. Guertin<sup>a</sup>, F. Haddad<sup>a,b</sup>, N. Michel<sup>a,b</sup>, V. Métivier<sup>a</sup>

<sup>a</sup>*SUBATECH, Ecole des Mines de Nantes, Université de Nantes, CNRS/IN2P3, Nantes, France*

<sup>b</sup>*GIP Arronax, 1 rue Aronax, 44817 Saint-Herblain, France*

---

## Abstract

### HIGHLIGHTS

- Deuteron induced reactions on natural titanium up to 34 MeV.
- Monitor reactions database (CRP IAEA).
- Experimental values determined using the stacked-foil technique.
- Comparison with the TALYS code version 1.6.

### ABSTRACT

Experimental cross sections for deuteron induced nuclear reactions on natural titanium were measured, using the stacked-foil technique and gamma spectrometry, up to 34 MeV with beams provided by the ARRONAX cyclotron. The experimental cross section values were monitored using the  $^{nat}\text{Ti}(d,x)^{48}\text{V}$  reaction, recommended by the IAEA. The excitation functions for  $^{nat}\text{Ti}(d,x)^{44m,46,47,48}\text{Sc}$  are presented and compared with the existing ones and with the TALYS 1.6 code calculations using default parameters. Our experimental values are in good agreement with data found in the literature. TALYS 1.6 is not able to give a good estimation of the production cross sections investigated in this work. These production cross sections of scandium isotopes fit on the new Coordinated Research Project (CRP) launched by the International Atomic Energy Agency (IAEA) to expand the database of monitor reactions.

---

*Email address:* [Charlotte.Duchemin@subatech.in2p3.fr](mailto:Charlotte.Duchemin@subatech.in2p3.fr) (C. Duchemin)

*Keywords:* stacked-foil technique, monitor reactions, deuteron beam,  $^{nat}\text{Ti}(\text{d},\text{x})$ , TALYS 1.6

---

## 1. Introduction

In the field of the production of medical radionuclides for diagnosis and therapy, it is important to be able to obtain always the same product quality. It is then necessary to keep control on the production of impurities during the irradiation. One key is to precisely know the production cross section, as a function of the incident particle energy, of all radionuclides produced in the target.

At the ARRONAX cyclotron (Haddad et al., 2008), the cross sections of different radionuclides for  $\beta$ - and  $\alpha$  targeted radionuclide therapy have been measured (Duchemin et al., 2015 a, Duchemin et al., 2015 b) using the stacked-foil technique (Blessing et al., 1995), which consists in the irradiation of a group of thin foils, and gamma spectrometry activity measurements. As sometimes deuteron beams give higher cross section values than proton beams on a same target (Guertin et al., 2014), we have focused some of our studies on the possible use of this projectile in the frame of the production of radionuclides for medical applications.

During our experiments, several stacks devoted to the determination of the production cross section of radioisotopes of medical interest as  $^{186\text{g}}\text{Re}$  (Duchemin et al., 2015 a),  $^{230}\text{Pa}$  (Duchemin et al., 2015 b) and  $^{155}\text{Tb}$ , were irradiated. Behind each target foil, titanium foils were included as monitor foils in order to take advantage of the excitation function of  $^{nat}\text{Ti}(\text{d},\text{x})^{48}\text{V}$  reaction which is well known and described (Tárkányi et al., 2001) in our energy range (up to 34 MeV). From the irradiation of titanium by deuterons several scandium isotopes can be produced and their production cross sections have been extracted.

Among these isotopes, some of them are used for medical applications as  $^{44\text{m/g}}\text{Sc}$  (Huclier-Markai et al., 2011),  $^{47}\text{Sc}$  (Majkowska-Pilip and Bilewicz, 2011) and the generator system  $^{44}\text{Ti}/^{44\text{g}}\text{Sc}$  (Pruszynski et al., 2010). In addition, titanium is increasingly used for nuclear, chemical, biomedical and aerospace applications due to its appropriate properties describe in the paper of Ravi Shankar et al., published in 2013. A good knowledge of the material activation due to its irradiation is then of great interest on these fields.

In addition, the International Atomic Energy Agency (IAEA) has initiated in 2012 a new Coordinated Research Project (CRP) to expand the

database of monitor reactions (Capote et al., 2012-2016).  $^{nat}\text{Ti}(d,x)^{46}\text{Sc}$  is one of the reaction identified by this project due to the  $^{46}\text{Sc}$  long half-life and its easily detectable gamma rays. Some other scandium isotopes may also be of interest as exposed in the following sections of this article.

## 2. Materials and methods

### 2.1. Experimental set-up and data measurements

At the ARRONAX cyclotron (Haddad et al., 2008), the cross section measurements are made using the stacked-foil method (Duchemin et al., 2015 a, Blessing et al., 1995) which consists in the irradiation of a set of thin foils, grouped as patterns. Each pattern contains a target to produce the isotopes of interest, a monitor foil to have information on the beam flux through the use of a reference reaction recommended by the International Atomic Energy Agency and a degrader to change the incident beam energy which comes in the other target foils. In this work, scandium isotopes are produced on natural abundance titanium foils provided by GoodFellow, with a chemical purity  $\chi$  of 99.6 %. These titanium foils were included as monitor foils in several stacks. Twenty stacks were irradiated, containing one to nine titanium foils in each, depending on the experiment. These stacks were devoted to the determination of the production cross section of radioisotopes of medical interest as  $^{186g}\text{Re}$  (Duchemin et al., 2015 a),  $^{230}\text{Pa}$  (Duchemin et al., 2015 b) and  $^{155}\text{Tb}$ . Each foil has been weighed before irradiation using an accurate scale ( $\pm 10^{-5}$  g) and scanned to precisely determine its area. From these values and assuming that the thickness is homogenous over the whole surface, the thickness is deduced. In average the thickness of the titanium foils is  $9.87 \mu\text{m}$  with a standard deviation of  $0.16 \mu\text{m}$ , and a mean uncertainty on the thickness of  $0.06 \mu\text{m}$ . The ARRONAX cyclotron can deliver protons up to 70 MeV, deuterons up to 34 MeV and alphas with an energy of 67.4 MeV (Haddad et al., 2008). The deuteron beam energy uncertainty is  $\pm 0.25$  MeV, as specified by the cyclotron provider, using simulations. The beam line is closed using a  $75 \mu\text{m}$  thick kapton foil which makes a barrier between the air in the vault and the vacuum in the line. The stacks were located about 7 cm downstream in air. The energy through each thin foil was determined in the middle of the thickness of the foil using the SRIM software (Ziegler et al., 2010). Energy loss in the kapton foil and air were taken into account. All along the stack, depending on the number of foils, the energy uncertainty calculated using the SRIM software increases up to 1.2 MeV

due to straggling and initial beam spread. Several stacks were irradiated with different incident energy in order to minimize this energy dispersion and cover the energy range from 34 MeV down to 6 MeV, which corresponds to the whole energy range of interest. Typical irradiations were carried out with a mean beam intensity of 107.5 nA (with a standard deviation of 44.9 nA) during 30 minutes. For all the experiments, the recommended cross section of the  $^{nat}\text{Ti}(d,x)^{48}\text{V}$  reaction (Tárkányi et al., 2001) is used to measure the particle flux. A Faraday cup was placed after the stack to control the intensity during the irradiation. The activity measurements in each foils were performed using a high purity germanium detector from Canberra (France) with low background lead and copper shielding, passing through a quality control once a week. All foils were counted twice. After one evening and night of decay (around 14 hours), the first activity measurements were performed for a duration of one hour and the second ones were performed for a minimum of 24 hours (one day) and up to 60 hours (during the week-end), after three weeks, waiting for the complete decay of Scandium-48. Indeed,  $^{48}\text{Sc}$  ( $T_{1/2} = 43.67$  (9) hours) has common gamma lines with the radioisotope of reference, Vanadium-48 ( $T_{1/2} = 15.9735$  (25) days). Nuclear data associated to  $^{48}\text{V}$  are summarized in Table 1.

Table 1: Vanadium-48 half-life and main  $\gamma$  rays (National Nuclear Data Center)

Radioisotope	$T_{1/2}$ (days)	$E_\gamma$ (keV)	$I_\gamma$ (%)
$^{48}\text{V}$	15.9735 (25)	944.130	7.870 (7)
		983.525	99.98 (4)
		1312.106	98.2 (3)

Gamma spectra were recorded in a suitable geometry calibrated in energy and efficiency with standard  $^{57,60}\text{Co}$  and  $^{152}\text{Eu}$  gamma sources from LEA-CERCA (France). The full widths at half maximum were 1.04 keV at 122 keV ( $^{57}\text{Co}$   $\gamma$  ray) and 1.97 keV at 1332 keV ( $^{60}\text{Co}$   $\gamma$  ray). Samples were placed at a height of 19 cm from the detector in order to reduce the dead time and the effect of sum peaks. The dead time during the counting was always kept below 10 %. The activity values of the produced radionuclides were derived from the spectra and the nuclear decay data given in Tables 1 and 2, using the FitzPeaks Gamma Analysis and Calibration Software (JF Computing Services).

## 2.2. Cross section calculation

Production cross section values can be determined from the activation formula in Eq. (1) using the appropriate projectile flux  $\Phi$ .

$$\sigma = \frac{Act \cdot A}{\chi \cdot \Phi \cdot N_a \cdot \rho \cdot e_f \cdot (1 - e^{-\lambda t})} \quad (1)$$

In this equation, the production cross section  $\sigma$  of a radioisotope depends on its measured activity reported to the end of irradiation ( $Act$ ), its decay constant ( $\lambda$ ), the target thickness ( $e_f$ ), its atomic number ( $A$ ), its density ( $\rho$ ) and its chemical purity ( $\chi$ ), the irradiation duration ( $t$ ) and the projectile flux ( $\Phi$ ).

In this work, the scandium isotopes and the  $^{48}\text{V}$  monitor are produced in the same foils, and receive the same flux. It is then easier to use the relative equation (2) in which the knowledge of the projectile flux is no longer necessary, thanks to the measured activity of  $^{48}\text{V}$  and its recommended cross section. In this equation, the prime parameters are associated to  $^{48}\text{V}$  while the others relate to scandium isotopes.

$$\sigma = \sigma' \cdot \frac{\chi' \cdot Act \cdot A \cdot \rho' \cdot e_f' (1 - e^{-\lambda' t})}{\chi \cdot Act' \cdot A' \cdot \rho \cdot e_f (1 - e^{-\lambda t})} \quad (2)$$

In the present case, where both radioisotopes are produced in the same foil, the production cross section is a function of the recommended  $^{48}\text{V}$  cross section, the  $^{48}\text{V}$  activity and scandium activity, only. The investigated scandium cross section can be calculated following the Eq. 3.

$$\sigma = \sigma' \cdot \frac{Act \cdot (1 - e^{-\lambda' t})}{Act' \cdot (1 - e^{-\lambda t})} \quad (3)$$

The cross section uncertainty is estimated with a propagation error calculation. Since all the parameters of equation (3) are independent, the total error is expressed as a quadratic form (Eq. (4)).

$$\frac{\Delta\sigma}{\sigma} = \sqrt{\left(\frac{\Delta\sigma'}{\sigma'}\right)^2 + \left(\frac{\Delta Act}{Act}\right)^2 + \left(\frac{\Delta Act'}{Act'}\right)^2} \quad (4)$$

The main error sources come from the recommended cross section  $\sigma'$  (around 12%),  $^{44m,46,47}\text{Sc}$  activity (up to 12%),  $^{48}\text{Sc}$  activity (up to 20%) and  $^{48}\text{V}$  activity (less than 2%). The contribution of the uncertainty on the irradiation time is not significant and has been neglected.

### 2.3. Comparison with the TALYS 1.6 code

In this work, all the experimental cross section values are compared with the latest version (1.6) of the TALYS code released in December, 2013 (Konig and Rochman, 2012). TALYS is a nuclear reaction program to simulate reaction induced by light particles on nuclei heavier than carbon. It incorporates many theoretical models to predict observables including theoretical cross section values as a function of the incident particle energy (from 1 keV to 1 GeV). Parameters are associated to these models in the input file. A combination of parameters that better describes the whole set of data available for all projectiles, targets and incident energies have been defined by the authors and put as default in the code. This way, the code can be launched with minimum information in the input file: the projectile type and its incident energy, the target type and its mass. The experimental data obtained in this work are compared to TALYS with default parameters (named TALYS 1.6 Default in the graphs).

## 3. Results

The following data on scandium radioisotopes come from the analysis of monitor titanium foils used in experiments devoted to the measure of the production cross section of radioisotopes of medical interest (Duchemin et al., 2015 a, Duchemin et al., 2015 b). All the experiments were, then, optimized to get a precise measurement of these radio-isotopes of medical interest and several hours of cooling time were needed. This leads us to loose informations on  $^{43,44g}\text{Sc}$  isotopes produced in the titanium monitor foils, both suitable for peptide radiolabelling for PET (Severin et al., 2013), which have short half-lives (less than 4 hours).

### 3.1. Production of $^{44m}\text{Sc}$

The  $^{44m}\text{Sc}$  has a half-life of  $T_{1/2} = 58.6$  (1) h. It decays by Electron Capture (EC) process (1.20 (7) %) to  $^{44}\text{Ca}$  (stable) by emitting three  $\gamma$  rays of 1001.83 (1.20%), 1126.06 (1.20%) and 1157.00 keV (1.20%).

It decays by Internal Transition (IT), at 98.80 (7) %, to its short-live ground state  $^{44g}\text{Sc}$  ( $T_{1/2} = 3.97$  (4) h) by emitting an intense  $\gamma$  ray at 271.13 keV (Table 2). The high branching ratio of this gamma line is used to extract the  $^{44m}\text{Sc}$  production cross section plotted in Figure 1. Our values are presented as full circles. These results are compared with data from the literature (Khandaker et al., 2013; Gagnon et al., 2010; Hermanne et al.,

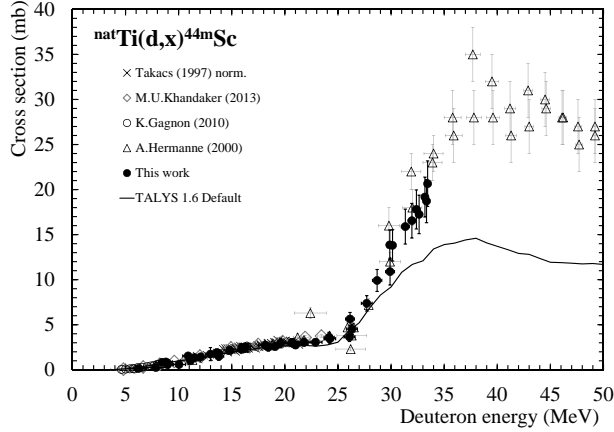


Figure 1: Experimental cross section of  $^{nat}\text{Ti}(d,x)^{44m}\text{Sc}$

2000; Takács et al., 1997) and the TALYS 1.6 code calculations (Koning and Rochman, 2012).

A good agreement with the previous experiments is observed up to 25 MeV. From 25 MeV, only A. Hermanne et al., 2000, obtained results and our data permit to confirm it, taking into account the uncertainties on both data set. The TALYS code gives satisfactory results for the lower energy part but underestimates the cross section above 25 MeV.

$^{44m}\text{Sc}$  can be a good candidate for monitor reaction due to its half-life higher than 2 days and its easily detectable gamma line which facilitates the activity measurement.

### 3.2. Cumulative production of $^{46}\text{Sc}$

$^{46}\text{Sc}$  has a ground state  $^{46g}\text{Sc}$  and a metastable state  $^{46m}\text{Sc}$ .  $^{46m}\text{Sc}$ , with a very short half-life ( $T_{1/2} = 18.75$  (4) s), decays by IT (100 %) to  $^{46g}\text{Sc}$  by emitting an intense  $\gamma$  ray of 142.528 keV. The half-life of the  $^{46m}\text{Sc}$  is so short, that, at the time of the activity measurements, all the  $^{46m}\text{Sc}$  has decayed into  $^{46g}\text{Sc}$ . It follows that we have been able to measure only the cumulative cross section  $^{46m+g}\text{Sc}$ . The  $^{46g}\text{Sc}$  gamma lines used to determine the  $^{46g}\text{Sc}$  activity are summarized in Table 2. The cross section results are collected in Table 3 and represented in Figure 2 with data from literature.

$^{46}\text{Sc}$  is proposed as new monitor reaction by the IAEA (Capote et al., 2012-2016) because of its relatively high cross section and its long half-life ( $T_{1/2} = 83.79$  (4) d). The Figure 2 shows that the  $^{46}\text{Sc}$  production cross

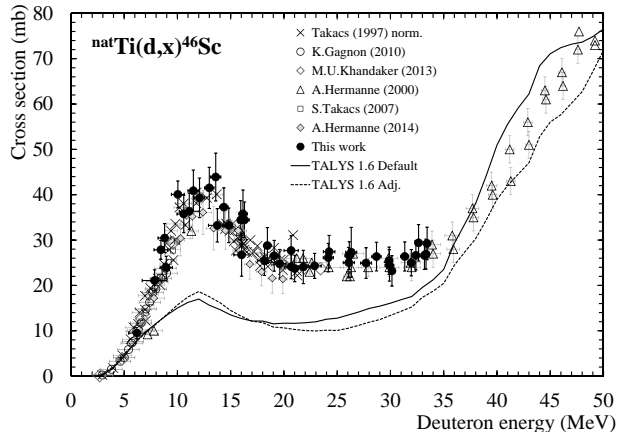


Figure 2: Experimental cross section of  $^{nat}\text{Ti}(d,x)^{46}\text{Sc}$

section has a maximum around 38 mbarn at 12 MeV for the lower energy part. This value is confirmed by several experiments including this work and the recent results of Khandaker et al., 2013 and Hermanne et al., 2014. Our experimental data come confirm the values of Hermanne et al., 2000, from 25 MeV, taking into account the uncertainties on the cross section values for both data set. The TALYS code doesn't permits to have a good estimation of the  $^{46}\text{Sc}$  production cross section up to 35 MeV. From this energy, TALYS results follow the only one experimental data set available, published by Hermanne et al., 2000.

### 3.3. Production of $^{47}\text{Sc}$

$^{47}\text{Sc}$  has a half-life of  $T_{1/2} = 3.3492(6)$  d. It decays by  $\beta$ - process at 100% to  $^{47}\text{Ti}$  (stable) emitting an intense  $\gamma$  ray at 159.377 keV (cf. Table 2). This  $\gamma$  line is used to derive the  $^{47}\text{Sc}$  activity from the  $\gamma$  spectra. The cross section values are plotted in Figure 3.

Up to 23 MeV, the results coming from all experiments are in good agreement. For these energies, the TALYS results are able to reproduce the experimental ones. Above 23 MeV, the results of this work confirm the data set published by Hermanne et al., 2000 and show that the TALYS code overestimates the cross section.

$^{47}\text{Sc}$ , in addition to be a good candidate to monitor reactions, is particularly promising for  $\beta$ - targeted therapy (Majkowska-Pilip and Bilewicz, 2011). The  $^{47}\text{Sc}$  production cross section is higher with deuterons than with protons

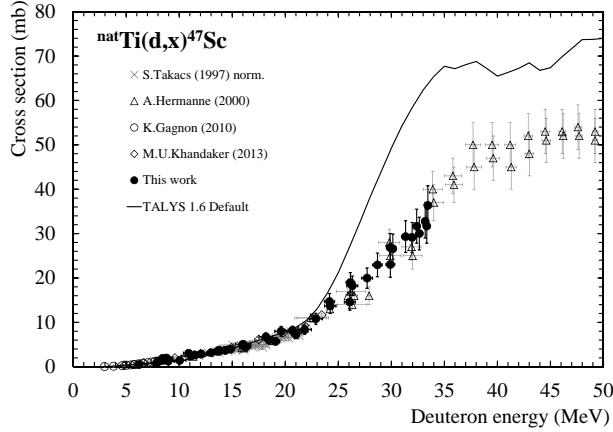


Figure 3: Experimental cross section of  $^{nat}\text{Ti}(d,x)^{47}\text{Sc}$

(Michel et al., 1978). But, in both case, the irradiation of a natural titanium foil leads to the production of the long half-life contaminant :  $^{46}\text{Sc}$ . Looking at the threshold values summarized in Table 2,  $^{47}\text{Sc}$  can be produced without  $^{46}\text{Sc}$  using a  $^{50}\text{Ti}$  target irradiated by deuteron between 5 and 15 MeV. Based on TALYS 1.6, the cross section of the reaction  $^{50}\text{Ti}(d,\alpha+n)^{47}\text{Sc}$  is around 30 mb at 15 MeV.

### 3.4. Production of $^{48}\text{Sc}$

$^{48}\text{Sc}$ , with a half-life of  $T_{1/2} = 43.67$  (9) h, decays to  $^{48}\text{Ti}$  (stable) by  $\beta$ - at 100%. It emits three  $\gamma$  lines with a branching ratio higher than 97 % at 983.526, 1037.522 and 1312.120 keV, and a  $\gamma$  line with a lower intensity at 175.361 keV (7.48 (10) %). In Table 2, only two gamma lines are summarized which correspond to those used to determine the  $^{48}\text{Sc}$  activity. The reason is that  $^{48}\text{V}$  ( $T_{1/2} = 15.9735$  (25) d) is also produced in the titanium target and emits two  $\gamma$  lines at 983.526 and 1312.120 keV which makes interferences with  $^{48}\text{Sc}$  gamma lines. The  $^{48}\text{Sc}$  production cross section is represented in Figure 4.

The values of this work are in good agreement with the literature data. However, the TALYS code results show a peak between 20 and 25 MeV which is not visible in the experimental data.

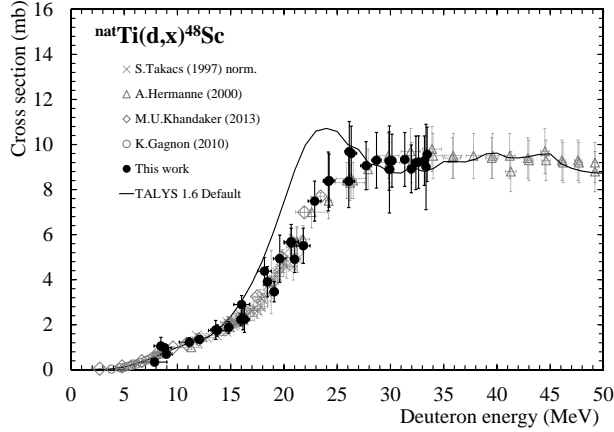


Figure 4: Experimental cross section of  $^{nat}\text{Ti}(d,x)^{48}\text{Sc}$

#### 4. Conclusion

Experimental cross sections for the  $^{nat}\text{Ti}(d,x)^{44m,46,47,48}\text{Sc}$  reactions, up to 34 MeV, have been extracted. The values were obtained from titanium foils included as monitor foils in stacked-foil experiments performed to obtain data on radioisotopes of medical interest such as  $^{186g}\text{Re}$  (Duchemin et al., 2015 a),  $^{230}\text{Pa}$  (Duchemin et al., 2015 b) and  $^{155}\text{Tb}$ . The cross sections have been determined relative to the recommended  $^{nat}\text{Ti}(d,x)^{48}\text{V}$  monitor reaction. Our data sets have been compared with data available in the literature and are in good agreement. Our results permit to confirm the trend made by the only one data set available in the literature from 25 MeV, published by Hermanne et al., 2000. The  $^{nat}\text{Ti}(d,x)^{46}\text{Sc}$  reaction is particularly interesting since the IAEA want to include it as a new monitor reaction (Capote et al., 2012-2016). The  $^{nat}\text{Ti}(d,x)^{44m,47}\text{Sc}$  reactions can also be considered as reference, as their production cross sections are well described. In addition, their half-live and gamma emissions permit to determine their activity, with a good accuracy. The TALYS 1.6 code using default models is not able to reproduce the experimental values for the investigated  $^{nat}\text{Ti}(d,x)$  reactions, especially from 25 MeV.

#### Acknowledgments

The ARRONAX cyclotron is a project promoted by the Regional Council of Pays de la Loire financed by local authorities, the French govern-

ment and the European Union. This work has been, in part, supported by a grant from the French National Agency for Research called "Investissements d'Avenir", Equipex Arronax-Plus n° ANR-11-EQPX-0004 and Labex n° ANR-11-EQPX-0018-01.

## References

Blessing, G., Bräutigam, W., Böge, H.G., Gad, N., Scholten, B., and Qaim, S.M., 1995. Internal irradiation system for excitation function measurement via the stacked-foil technique, *Appl. Radiat. Isot.* 955, 46-9.

Capote, R., IAEA project officer, Tarkanyi, F.T., - Chairman Reaction Data (Hungary), Nichols, A.L., - Chairman Decay Data (UK), Be, M.-M., (France), Carlson, B.V., (Brazil), Hussain, M., (Pakistan), Ignatyuk, A.V., (Russian Federation), Kim, G., (Korea), Kondev, F.G. (USA), Lebeda, O., (Czech Republic), Luca, A., (Romania), Nagai, T., (Japan), Naik, H., (India), Nortier, M., (USA), and Spahn, I., (Germany). Duration : 2012-2016. CRP on Nuclear Data for Charged-particle Monitor Reactions and Medical Isotope Production. CRP code : F4.10.29.

Duchemin, C., Guertin, A., Haddad, F., Michel, N., Métivier, V., 2015 a. Cross section measurements of deuteron induced nuclear reactions on natural tungsten up to 34 MeV, *Applied radiation and Isotopes* 97, 5258.

Duchemin, C., Guertin, A., Haddad, F., Michel, N., Métivier, V., 2015 b. Production of medical isotopes from a thorium target irradiated by light charged particles up to 70 MeV, *Phys. Med. Biol.* 60, 931946.

Ekström, L.F., and Firestone, R.B., 2004. Information extracted from the Table of Radioactive Isotopes, version 2.1.

FitzPeaks Gamma Analysis and Calibration Software version 3.66, produced by JF Computing Services (UK), based on methods presented in *Nucl.Instrum. and Methods* (1981) 190, 89-99, describing the program SAMPO80 of the Helsinki University of Technology, Finland.

Gagnon, K., Avila-Rodriguez, M.A., Wilson, J., McQuarrie, S.A., 2010. Experimental deuteron cross section measurements using single natural titanium foils from 3 to 9 MeV with special reference to the production of  $^{47}\text{V}$  and  $^{51}\text{Ti}$ , *Nucl. Instrum. Methods Phys. Res., Sect. B* 268, 1392-1398.

Guertin, A., Duchemin, C., Haddad, F., Michel, N., Métivier, V., 2014. Measurements of  $^{186}\text{Re}$  production cross section induced by deuterons on natW target at ARRONAX facility, *Nucl. Med. Biol.* 41, e16-e18.

Haddad, F., Ferrer, L., Guertin, A., Carlier, T., Michel, N., Barbet, J., Chatal, J.F., 2008. Arronax a high-energy and high-intensity cyclotron for nuclear medicine, *Eur. J. Nucl. Med. Mol. Imaging* 35, 1377-1387.

Hermanne, A., Sonck, M., Takács, S., Tárkányi, F., 2000. Experimental study of excitation functions for some reactions induced by deuterons (10-50 MeV) on natural Fe and Ti, *Nucl. Instrum. Methods Phys. Res., Sect. B* 161-163, 178-185.

Hermanne, A., Tárkányi, F., Takács, S., Ditrói, F., Amjed, N., 2014. Excitation functions for production of  $^{46}\text{Sc}$  by deuteron and proton beams in natTi: A basis for additional monitor reactions, Volume 338, Pages 3141.

Huclier-Markai, S., Sabatié, A., Ribet, S., Kubicek, V., Paris, M., Vidaud, C., Hermann, P., Cutler, C.S., 2011. Chemical and biological evaluation of scandium(III)-polyaminopolycarboxylate complexes as potential PET agents and radiopharmaceuticals, *Radiochim. Acta* 99, 653662.

Khandaker, M.U., Haba, H., Kanaya, J., Otuka, N., 2013. Excitation functions of (d,x) nuclear reactions on natural titanium up to 24 MeV, *Nucl. Instrum. Methods Phys. Res., Sect. B* 296, 14-21.

Koning, A.J., Rochman, D., 2012. Modern nuclear data evaluation with the TALYS code system, *Nucl. Data Sheets* 113, 2841.

Majkowska-Pilip, A., Bilewicz, A., 2011. Complexes of scandium radionuclides as precursors for diagnostic and therapeutic radiopharmaceuticals, *Journal of Inorganic Biochemistry* 105, 313320.

Michel, R., Brinkmann, G., Weigel, H., Herr, W., 1978. Proton-induced reactions on titanium with energies between 13 and 45 MeV, Volume 40, Issue 11, 18451851.

National Nuclear Data Center, information extracted from the Experimental Nuclear Reaction Data (EXFOR) Database <http://www.nndc.bnl.gov/exfor/exfor.htm>, Version of November 05, 2013.

Pruszyński, M., Loktionova, N.S., Filosofov, D.V., Rosch, F., 2010. Post-elution processing of  $^{44}\text{Ti}/^{44}\text{Sc}$  generator-derived  $^{44}\text{Sc}$  for clinical application, *Appl. Radiat. Isot.* 68, 16361641.

Ravi Shankar, A., Karthiselva, N.S., Kamachi Mudali, U., 2013. Thermal oxidation of titanium to improve corrosion resistance in boiling nitric acid medium. *Surface and Coatings Technology* 235, 4553.

Severin, G.W., Engle, J.W., Valdovinos, H.F., Barnhart, T.E., Nickles, R.J., 2012. Cyclotron produced  $^{44}\text{gSc}$  from natural calcium, *Appl. Radiat. Isot.* 70, 15261530.

Takács, S., Sonck, M., Scholten, B., Hermanne, A., Tárkányi, F., 1997.

Excitation functions of deuteron induced nuclear reactions on  $^{nat}\text{Ti}$  up to 20 MeV for monitoring deuteron beams, Appl. Radiat. Isot. 48-5, 657-665.

Tárkányi, F., Takács, S., Gul, K., Hermanne, A., Mustafa, M.G., Nortier, M., Oblozinsky, P., Qaim, S.M., Scholten, B., Shubin, Yu.N., Youxiang, Z., 2001. Beam monitor reactions, in Charged Particle Cross Section Database for Medical Radioisotope Production: Diagnostic Radioisotopes and Monitor Reactions; IAEA-TECDOC-1211, pages 49-152, IAEA, Vienna. Database available on <https://www-nds.iaea.org/medportal/>, update may 2013.

Ziegler, J.F., Ziegler, M.D., Biersack, J.P., 2010. SRIM The stopping and range of ions in matter, Nucl. Instrum. Methods Phys. Res., Sect. B 268, 1818-1823.

Table 2: Produced scandium radioisotopes parameters (Ekstrm and Firestone, 2004) and Q-value extracted from the National Nuclear Data Center.

Radioisotope	$T_{1/2}$	$E_\gamma$ (keV)	$I_\gamma$ (%)	Contributing reactions	Q value				
$^{44m}\text{Sc}$	58.6 (1) h	271.13	86.7 (3)	$^{46}\text{Ti}(d,\alpha)$	4.40				
				$^{46}\text{Ti}(d,n+^3\text{He})$	-16.18				
				$^{46}\text{Ti}(d,2d)$	-19.45				
				$^{46}\text{Ti}(d,2n+2p)$	-23.90				
				$^{47}\text{Ti}(d,n+\alpha)$	-4.48				
				$^{47}\text{Ti}(d,2n+^3\text{He})$	-25.06				
				$^{48}\text{Ti}(d,2n+\alpha)$	-16.11				
				$^{49}\text{Ti}(d,n+\alpha)$	-24.25				
				$^{46}\text{Sc}$	83.79 (4) d	889.277	99.984 (1)	$^{46}\text{Ti}(d,2p)$	-3.81
						1120.545	99.987 (1)	$^{47}\text{Ti}(d,^3\text{He})$	-4.97
								$^{47}\text{Ti}(d,n+2p)$	-12.69
								$^{48}\text{Ti}(d,\alpha)$	3.98
								$^{48}\text{Ti}(d,n+^3\text{He})$	-16.60
		$^{48}\text{Ti}(d,2d)$	-19.87						
$^{47}\text{Sc}$	3.3492 (6) d	159.377	68.3 (4)	$^{48}\text{Ti}(d,2n+2p)$	-24.32				
				$^{49}\text{Ti}(d,n+\alpha)$	-4.16				
				$^{49}\text{Ti}(d,2n+^3\text{He})$	-24.74				
				$^{50}\text{Ti}(d,2n+\alpha)$	-15.10				
				$^{47}\text{Ti}(d,2p)$	-2.04				
				$^{48}\text{Ti}(d,^3\text{He})$	-5.95				
				$^{48}\text{Ti}(d,n+2p)$	-13.67				
				$^{49}\text{Ti}(d,\alpha)$	6.48				
				$^{49}\text{Ti}(d,n+^3\text{He})$	-14.09				
				$^{49}\text{Ti}(d,2n+2p)$	-21.81				
$^{48}\text{Sc}$	43.67 (9) h	175.361	7.48 (9)	$^{50}\text{Ti}(d,n+\alpha)$	-4.46				
		1037.599	97.6 (5)	$^{50}\text{Ti}(d,2n+^3\text{He})$	-25.03				
				$^{48}\text{Ti}(d,2p)$	-5.43				
				$^{49}\text{Ti}(d,^3\text{He})$	-5.85				
				$^{49}\text{Ti}(d,n+2p)$	-13.57				
				$^{50}\text{Ti}(d,\alpha)$	3.78				
				$^{50}\text{Ti}(d,n+^3\text{He})$	-16.79				
		$^{50}\text{Ti}(d,2n+2p)$	-24.51						

Table 3: Experimental cross section values for  $^{nat}\text{Ti}(\text{d},\text{x})^{44\text{m},46,47,48}\text{Sc}$  reactions

Energy (MeV)	$\sigma^{44\text{m}}\text{Sc}$ (mb)	$\sigma^{46}\text{Sc}$ (mb)	$\sigma^{47}\text{Sc}$ (mb)	$\sigma^{48}\text{Sc}$ (mb)
$33.44 \pm 0.28$	$19.75 \pm 2.29$	$27.97 \pm 3.25$	$34.75 \pm 4.02$	$9.15 \pm 1.10$
$33.34 \pm 0.30$	$18.72 \pm 2.40$	$26.90 \pm 3.32$	$31.68 \pm 3.84$	$9.00 \pm 1.90$
$33.19 \pm 0.30$	$19.17 \pm 2.21$	$26.61 \pm 3.07$	$32.76 \pm 3.77$	$9.28 \pm 1.10$
$32.39 \pm 0.35$	$17.34 \pm 2.04$	$25.94 \pm 3.02$	$30.87 \pm 3.61$	$8.96 \pm 1.12$
$32.64 \pm 0.32$	$17.25 \pm 2.13$	$29.39 \pm 4.01$	$30.00 \pm 3.69$	$9.22 \pm 1.16$
$31.96 \pm 0.35$	$16.54 \pm 1.92$	$25.00 \pm 2.90$	$29.14 \pm 3.37$	$8.92 \pm 1.06$
$31.34 \pm 0.38$	$15.47 \pm 1.81$	$25.69 \pm 3.00$	$28.54 \pm 3.33$	$9.09 \pm 1.12$
$30.14 \pm 0.28$	$13.81 \pm 1.74$	$23.20 \pm 3.35$	$26.58 \pm 3.33$	$9.28 \pm 1.18$
$29.91 \pm 0.42$	$10.89 \pm 1.48$	$24.42 \pm 3.47$	$23.03 \pm 2.87$	$8.89 \pm 1.93$
$29.88 \pm 0.30$	$13.86 \pm 1.66$	$25.45 \pm 3.01$	$26.87 \pm 3.16$	$9.27 \pm 1.30$
$28.69 \pm 0.44$	$9.91 \pm 1.22$	$26.36 \pm 3.17$	$22.94 \pm 2.67$	$9.30 \pm 1.24$
$27.71 \pm 0.51$	$7.38 \pm 0.86$	$24.93 \pm 3.39$	$19.96 \pm 2.29$	$9.06 \pm 1.07$
$26.32 \pm 0.52$	$4.33 \pm 0.54$	$26.21 \pm 5.23$	$17.52 \pm 2.05$	$9.22 \pm 1.13$
$26.14 \pm 0.41$	$5.64 \pm 0.73$	$26.56 \pm 3.06$	$18.97 \pm 2.22$	$9.69 \pm 1.34$
$26.09 \pm 0.52$	$3.65 \pm 0.51$	$25.03 \pm 3.34$	$14.57 \pm 1.84$	$8.37 \pm 1.17$
$24.24 \pm 0.54$	$3.45 \pm 0.51$	$27.42 \pm 3.60$	$13.70 \pm 1.71$	$8.40 \pm 1.18$
$24.17 \pm 0.48$	$3.59 \pm 0.55$	$26.13 \pm 3.14$	$14.69 \pm 1.79$	$8.36 \pm 1.31$
$22.88 \pm 0.62$	$3.05 \pm 0.37$	$24.30 \pm 2.76$	$10.81 \pm 1.25$	$7.49 \pm 0.89$
$21.82 \pm 0.64$	$3.06 \pm 0.43$	$24.07 \pm 3.67$	$8.34 \pm 1.04$	$5.51 \pm 0.78$
$21.01 \pm 0.32$	$2.75 \pm 0.33$	$23.73 \pm 2.92$	$7.20 \pm 0.85$	$4.91 \pm 0.59$
$20.69 \pm 0.67$	$2.95 \pm 0.35$	$24.11 \pm 2.64$	$8.18 \pm 0.91$	$5.63 \pm 0.65$
$20.68 \pm 0.66$	$3.05 \pm 0.41$	$27.69 \pm 3.26$	$8.14 \pm 0.97$	$5.69 \pm 0.76$
$19.61 \pm 0.60$	$2.96 \pm 0.52$	$24.74 \pm 3.19$	$8.00 \pm 1.11$	$4.93 \pm 1.05$
$19.09 \pm 0.39$	$2.58 \pm 0.33$	$26.53 \pm 3.40$	$5.72 \pm 0.72$	$3.46 \pm 0.45$
$18.45 \pm 0.34$	$2.51 \pm 0.43$	$28.79 \pm 3.97$	$6.02 \pm 0.86$	$3.91 \pm 0.67$
$18.17 \pm 0.65$	$2.72 \pm 0.38$	$25.46 \pm 3.27$	$6.74 \pm 0.87$	$4.38 \pm 0.61$
$16.30 \pm 0.44$	$2.56 \pm 0.36$	$34.45 \pm 3.95$	$4.52 \pm 0.53$	$2.24 \pm 0.58$
$16.16 \pm 0.40$	$2.36 \pm 0.43$	$35.77 \pm 5.27$	$4.53 \pm 0.73$	$2.28 \pm 0.51$
$16.03 \pm 0.73$	$2.28 \pm 0.29$	$26.73 \pm 4.70$	$5.07 \pm 0.60$	$2.90 \pm 0.40$
$15.95 \pm 0.29$	$2.47 \pm 0.30$	$34.41 \pm 4.31$	$4.88 \pm 0.58$	$2.23 \pm 0.27$
$14.82 \pm 0.35$	$2.13 \pm 0.25$	$33.25 \pm 3.82$	$3.96 \pm 0.46$	$1.88 \pm 0.26$
$14.36 \pm 0.40$	$37.26 \pm 4.26$	$3.71 \pm 0.84$		

Table 4: Experimental cross section values for  $^{nat}\text{Ti}(\text{d},\text{x})^{44\text{m},46,47,48}\text{Sc}$  reactions

Energy (MeV)	$\sigma^{44\text{m}}\text{Sc}$ (mb)	$\sigma^{46}\text{Sc}$ (mb)	$\sigma^{47}\text{Sc}$ (mb)	$\sigma^{48}\text{Sc}$ (mb)
$13.75 \pm 0.83$	$1.84 \pm 0.23$	$33.24 \pm 3.68$	$3.76 \pm 0.44$	$1.75 \pm 0.25$
$13.60 \pm 0.48$	$1.91 \pm 0.35$	$43.90 \pm 5.28$	$3.46 \pm 0.55$	$1.77 \pm 0.42$
$13.00 \pm 0.44$	$1.74 \pm 0.72$	$41.51 \pm 4.54$	$3.15 \pm 0.45$	
$12.07 \pm 0.48$	$1.44 \pm 0.16$	$39.31 \pm 4.37$	$2.89 \pm 0.32$	$1.35 \pm 0.17$
$11.50 \pm 0.51$	$1.35 \pm 0.35$	$40.88 \pm 4.56$	$2.64 \pm 0.35$	
$11.11 \pm 0.95$	$0.99 \pm 0.14$	$32.02 \pm 3.59$	$2.42 \pm 0.30$	$1.23 \pm 0.20$
$10.60 \pm 0.64$		$35.75 \pm 4.13$		
$10.04 \pm 0.60$	$0.59 \pm 0.12$	$40.07 \pm 2.98$	$1.42 \pm 0.14$	
$8.96 \pm 0.57$	$0.57 \pm 0.07$	$23.94 \pm 2.51$	$1.24 \pm 0.13$	$0.69 \pm 0.10$
$8.80 \pm 0.62$	$0.87 \pm 0.09$	$30.45 \pm 3.18$	$1.96 \pm 0.20$	$0.98 \pm 0.11$
$8.45 \pm 0.65$	$0.83 \pm 0.17$	$27.85 \pm 2.08$	$1.91 \pm 0.27$	$1.06 \pm 0.39$
$7.86 \pm 1.16$	$0.25 \pm 0.04$	$21.08 \pm 2.36$	$0.72 \pm 0.10$	$0.34 \pm 0.06$
$6.20 \pm 0.77$	$0.14 \pm 0.03$	$9.48 \pm 1.23$	$0.46 \pm 0.06$	